RESEARCH ARTICLE

Life history scaling in a tropical forest

John M. Grady[1,2,3] | **Quentin D. Read**[2,4] | **Sydne Record**[3,5] | **Nadja Rüger**[6,7,8] | **Phoebe L. Zarnetske**[2,9] | **Anthony I. Dell**[1,10] | **Stephen P. Hubbell**[8,11] | **Sean T. Michaletz**[12,13,14] | **Brian J. Enquist**[12,15]

[1]Department of Biology, Washington University in St. Louis, St. Louis, Missouri, USA; [2]Ecology, Evolution, and Behavior Program, Michigan State University, East Lansing, Michigan, USA; [3]Department of Biology, Bryn Mawr College, Bryn Mawr, Pennsylvania, USA; [4]USDA Agricultural Research Service, Raleigh, North Carolina, USA; [5]Department of Wildlife, Fisheries, and Conservation Biology, University of Maine, Orono, Maine, USA; [6]German Centre for Integrative Biodiversity Research (iDiv) Halle-Jena-Leipzig, Leipzig, Germany; [7]Department of Economics, University of Leipzig, Leipzig, Germany; [8]Smithsonian Tropical Research Institute, Balboa, Panama; [9]Department of Integrative Biology, Michigan State University, East Lansing, Michigan, USA; [10]National Great Rivers Research and Education Center, East Alton, Illinois, USA; [11]Department of Ecology and Evolutionary Biology, University of California, Los Angeles, California, USA; [12]Department of Ecology and Evolutionary Biology, University of Arizona, Tucson, Arizona, USA; [13]Earth and Environmental Sciences Division, Los Alamos National Laboratory, Los Alamos, New Mexico, USA; [14]Department of Botany, University of British Columbia, Vancouver, British Columbia, Canada and [15]The Santa Fe Institute, Santa Fe, New Mexico, USA

Correspondence
John M. Grady
Email: jgradym@gmail.com

Handling Editor: Pieter Zuidema

Abstract

1. Both tree size and life history variation drive forest structure and dynamics, but little is known about how life history frequency changes with size. We used a scaling framework to quantify ontogenetic size variation and assessed patterns of abundance, richness, productivity and light interception across life history strategies from >114,000 trees in a primary, neotropical forest. We classified trees along two life history axes: a *fast–slow* axis characterized by a growth–survival trade-off, and a *stature–recruitment* axis with tall, *long-lived pioneers* at one end and short, *short-lived recruiters* at the other.

2. Relative abundance, richness, productivity and light interception follow an approximate power law, systematically shifting over an order of magnitude with tree size. *Slow* saplings dominate the understorey, but *slow* trees decline to parity with rapidly growing *fast* and *long-lived pioneer* species in the canopy.

3. Like the community as a whole, *slow* species are the closest to obeying the energy equivalence rule (EER)—with equal productivity per size class—but other life histories strongly increase productivity with tree size. Productivity is fuelled by resources, and the scaling of light interception corresponds to the scaling of productivity across life history strategies, with *slow* and *all* species near solar energy equivalence. This points towards a resource-use corollary to the EER: the resource equivalence rule.

4. Fitness trade-offs associated with tree size and life history may promote coexistence in tropical forests by limiting niche overlap and reducing fitness differences.

5. *Synthesis*. Tree life history strategies describe the different ways trees grow, survive and recruit in the understorey. We show that the proportion of trees with a pioneer life history strategy increases steadily with tree size, as pioneers become

relatively more abundant, productive, diverse and capture more resources towards the canopy. Fitness trade-offs associated with size and life history strategy offer a mechanism for coexistence in tropical forests.

KEYWORDS
coexistence, energy equivalence, life history, niche, scaling, tropical forests

1 | INTRODUCTION

Tree life histories are a major component of trait variation that provides insight into how tropical forests are assembled, including changes in species composition and biomass over time (Rüger et al., 2020). The most well-known life history dimension in trees is a *growth–survival* trade-off that underlies a widespread *fast–slow* life history axis in mesic forests, in which fast-growing, but short-lived pioneer species ('*fast*') regenerate in disturbances or gaps from treefalls (Reich, 2014; Wright et al., 2010). Conversely, species with slow growth but low mortality ('*slow*') tolerate shade and often dominate late successional forests. More recently, Rüger et al. (2018) synthesized recruitment, growth and mortality rates at different size stages to reveal an additional life history axis characterized by a *stature–recruitment* trade-off. *Long-lived pioneers* (*LL pioneers*) with poor recruitment and large maximum size occupy one end of the continuum, and small, short-lived shrubs and understorey trees that recruit well occupy the other end (*SL recruiters*). In some forests, *LL pioneers* represent a large portion of carbon stores due, in part, to their massive size, as tree biomass generally increases in larger size classes (Lutz et al., 2018; Rüger et al., 2020). Indeed, tree size is a well-known driver of forest structure: governing patterns of abundance, mortality, carbon storage and carbon sinks (Hubau et al., 2019; Niklas, 1994; West et al., 2009). Tree size is often an important categorical component of life history classification (e.g. Rüger et al., 2018), but how life history frequency changes continuously with size has received less attention. For instance, pioneer species are often regarded as a relatively small component of mature forests (Molino & Sabatier, 2001; Whitmore, 1984), but their rarity may be size-dependent. Numerical assessment of tree abundance are effectively a measure of saplings, which are orders of magnitude more common than canopy trees. If pioneer species outgrow *slow* species and increase in relative frequency with size, they would constitute a progressively larger proportion of canopy composition, forest biomass and carbon sequestration (Condit et al., 1998; Lima et al., 2016).

A scaling approach to life histories is useful for quantifying how traits change continuously with size. Many aspects of physiological rates and demography change or scale as an allometric function of organismal size following a power law: $y \propto x^{\alpha}$, where y is a quantity, x is organismal size (e.g. stem diameter) and α is a scaling exponent $\neq 1$ that is the slope on a log–log plot. Tree abundance per area, for instance, often follows an approximate power law with tree size in forest communities (Niklas, 2004), although some departure from a power law at upper or lower size limits is common. Muller-Landau, Condit, Harms, et al. (2006) showed that size distributions emerge

from individual growth and mortality rates. Condit et al. (1998) found that fast-growing species maintained low abundances in the understorey because they quickly grew out of small size classes. Therefore, we expect slow-growing and shade-tolerant *slow* trees to be the most common at small sizes but become proportionally less abundant at larger classes, as fast-growing *fast* and *LL pioneers* outpace them (Figure 1a). Further, if richness is an allometric function of abundance, as observed in some systems (McClain, 2004), we expect richness to also scale with tree size in a similar fashion, albeit with shallower slopes (Figure 1c). Note that differences in scaling slopes of abundance or richness between life histories imply a proportional shift of life history frequency from the understorey to the top of the canopy. Specifically, differences in scaling slopes between different life history strategies are equivalent to regressing the ratio of response variables from two life history strategies against size. This provides a convenient metric for the rate of relative (per-stem) change in abundance and richness with tree size (Figure 1b,d).

A scaling approach to life history frequency can also shed light on the theoretical underpinnings of forest structure. A widespread feature of ecosystems, from algae to forests, is that the scaling of organismal metabolism offsets with the scaling of population abundance such that many small organisms collectively respire as much as a few large ones. In particular, if R is metabolic rate, S is organismal size, A is abundance per area and RA is the total metabolic rate, $R \propto S^{\alpha}$, $A \propto S^{-\alpha}$ and $RA \propto S^{0}$. This implies that all individuals at a given size collectively flux equal amounts of metabolic energy as other size classes, a phenomenon known as the energy equivalence rule (EER). The EER has been argued to be an organizing feature of communities, linking individual metabolism to community scale patterns (Damuth, 1998; Deng et al., 2008; Perkins et al., 2019; West et al., 2009). Although there is site-to-site deviation, the EER appears to be a macroecological average across forests and other autotrophic systems (Perkins et al., 2019; Zhang et al., 2015). There is little understanding, however, of how functional trait variation *within* communities reflects or deviates from whole-community EER. Because metabolism is fuelled by resources, deviation from EER may reveal how trees with different life history strategies compete for resources at different sizes. We expect that scaling shifts in relative abundance (Figure 1b) will lead to departure from EER, particularly in fast-growing *fast* and *LL pioneers* that initially constitute only a small fraction of the understorey. Specifically, we predict *fast* and *LL pioneers* will deviate from EER by progressively increasing their share of resources and metabolic flux at larger size classes (Figure 1e,f).

Finally, shifts in the relative frequency of tree life histories with size may also inform a longstanding debate in ecology: how trait
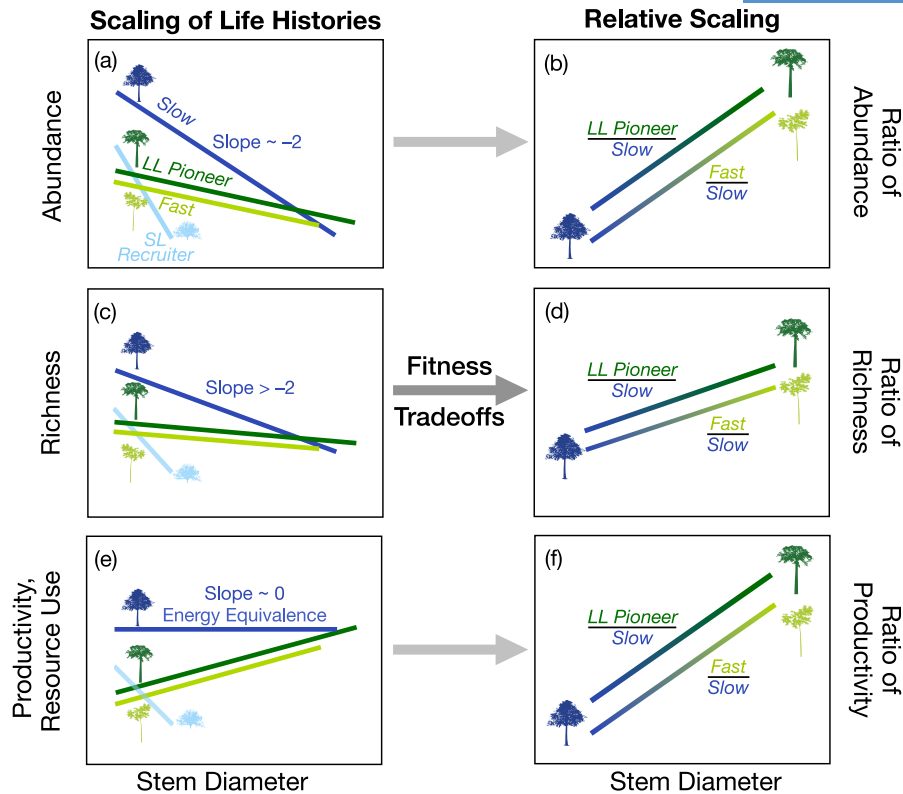
Scaling of Life Histories

Relative Scaling

FIGURE 1 A schematic for life history scaling with tree size. Different scaling slopes of abundance per area (a), richness (c) and productivity/resource use (e) lead to proportional shifts with size across life history strategies (b, d, f). In particular, in b, d and f we plot the corresponding dimensionless ratio of relative abundance, richness and productivity/resource use between distinct life history strategies that reach the canopy: *fast*, *slow* and *long-lived* (*LL*) *pioneers*. Shade-tolerant slow saplings are predicted to dominate the understorey (highest *y*-intercept) but decline rapidly as fast-growing *fast* and *LL pioneer* species become increasingly common towards the canopy; other *y*-intercepts are arbitrary. Richness scaling (c) is predicted to track abundance (a), but with shallower slopes. Shade-tolerant *slow* species are expected to be the closest to equivalent productivity per stem size (e, 'energy equivalence'). Productivity is fuelled by resource use, so both are expected to show similar scaling patterns for collective rates of resource use like light interception (e). Because *medium* trees are intermediate in trait space we do not include a scaling prediction. All axes are log-transformed. See Figure S1 in Supporting Information S1 for life history principal component analysis values.

variation promotes species diversity. Because *fast-slow* life history variation in humid forests corresponds to shade tolerance and recruitment success (Rüger et al., 2018; Valladares & Niinemets, 2008), it has long been thought that variation in life history may promote the partitioning of light in the understorey, reducing niche overlap and promoting coexistence (Ricklefs, 1977; Whitmore, 1989). The partitioning of light across tree gapfalls—which can lead to over an order of magnitude of variation in light availability—has been of particular interest. Hubbell et al. (1999) reasoned that niche differences between pioneers and shade-tolerant species should lead to changes in the relative richness of these groups as a function of their proximity to gaps. But in analyses of diverse, primary forests in the neotropics, Hubbell et al. (1999) at Barro Colorado Island (BCI), Panama, and Lieberman et al. (1995) at La Selva, Costa Rica, failed to find any difference in per-stem richness between shade-tolerant and pioneer species in understorey gaps and non-gaps (but see Molino & Sabatier, 2001; Terborgh et al., 2017). Similar findings have been reported in a diverse, primary temperate forest (Busing & White, 1997). A review by Brokaw and Busing (2000) concluded

that 'gaps help maintain species diversity mostly by harboring higher densities of stems, not by providing more niches'.

However, the most sustained, non-stochastic changes in light intensity—where light limitation, differential growth and mortality should be most pronounced and persistent—is with tree size over ontogeny, as light intensity increases more than two orders of magnitude from the forest floor to the canopy (Muller-Landau, Condit, Chave, et al., 2006; Stark et al., 2012). A variety of mortality stressors also shift with ontogenetic size: relative humidity and leaf fungal load decline with size while water stress, wind-throw and lightning strike frequency increase towards the canopy (Bennett et al., 2015; Canham et al., 2001; Gilbert et al., 2007; Gora et al., 2020; Madigosky, 2004). Thus, variation in per-stem richness across life history strategies may be more apparent as a function of tree size, rather than across gaps or light availability in the understorey.

Niche theory posits that coexistence of species A and B occurs when intra-specific competition exceeds inter-specific competition (Chesson, 2000). This may occur when species A outperforms species B in one environment, but species B outperforms

species A in another (Kitajima & Poorter, 2008; Silvertown, 2004). Microenvironments, such as light availability, change with tree size and both theoretical and empirical work indicate that species with overlapping ontogenetic sizes can coexist by having fitness advantages at different size stages such that total intra-specific variation over ontogeny exceeds total inter-specific variation (Baraloto et al., 2005; Bassar et al., 2017; Kitajima & Poorter, 2008; Kohyama & Takada, 2012). In forests, one mechanism argued to promote size-based niche partitioning is variation in tree crown structure, which varies with life history strategy and impacts competitors asymmetrically with size by reducing light to smaller competitors but not larger (Iida et al., 2011; Poorter et al., 2006; Turner, 2001). Crown variation has been analytically shown to permit stable niche partitioning (Kohyama & Takada, 2012) and Bohlman and O'Brien (2006) found that shade-tolerant species have larger, deeper crowns than gap species at our study site in BCI, Panama.

A second way fitness trade-offs with size can maintain diversity is by reducing whole organismal fitness differences between species when trade-offs are integrated over ontogeny. As species become more competitively similar, rates of exclusion decline, helping to maintain standing diversity (Chesson, 2000; Hubbell, 2005). In trees, performance trade-offs have been documented in reversals of relative growth rate and survival rank in seedlings over ontogeny (Baraloto et al., 2005), though this pattern may not be widespread (Kitajima & Poorter, 2008). Because growth rate and survival are typically negatively correlated, integrating these performance measures is an important challenge (Kitajima & Poorter, 2008). At the demographic level, we suggest that scaling shifts in relative abundance—which is a function of growth and mortality (Muller-Landau, Condit, Harms, et al., 2006) and can be regarded as a proxy for fitness (Álvarez-Yépiz et al., 2017; Shipley et al., 2016)—represent a direct and more integrative measure of performance trade-offs that reduce fitness differences. Although the hyper species diversity of tropical forests is unlikely to solely reflect life history variation (Condit et al., 2006), we suggest that consistent functional diversity and associated richness in humid forests may be maintained, in part, by fitness trade-offs with size and life history strategy that promote coexistence.

1.1 | The scaling of life histories and light interception

We use a scaling framework to test four predictions. First, we predict increases in the relative abundance, richness and above-ground woody productivity of *fast* and *LL pioneers* relative to *slow* species, which overlap in ontogenetic size. We define above-ground woody productivity (hereafter 'productivity', *P*) as the sum of individual above-ground woody growth rate ('mass growth', *G*) per hectare per unit stem diameter ($kg\,year^{-1}\,ha^{-1}\,cm^{-1}$). Note that while differences in maximum tree size may promote coexistence (Kohyama et al., 2015), we are particularly interested in demographic shifts occurring in species with overlapping ontogenetic sizes and contrasting life histories (Figure 1; Figure S1). For this reason, we give special

attention to relative scaling differences between canopy-reaching *fast*, *slow* and *LL pioneers* (Figure 1b,d,f). Categorical life history groups have a long history of discussion, spurring our use here, but these groupings occur along a continuum. For this reason, we also test the prediction that average life history principal component analysis (PCA) loadings shift with tree size and light intensity from *slow* and *SL recruiters* in the shade/understorey, towards *fast* and *LL pioneers* in high light/canopy.

Second, we predict that richness, like abundance, is an allometric function of tree size (Figure 1c). If richness is driven by abundance, we expect a power relationship between the richness and abundance. We compare scaling slopes of abundance and richness with size and also regress richness against abundance and determine if slopes are <1.

Third, we predict that at the whole-community scale, an undisturbed forest is close to the EER with respect to productivity, characterized by a slope of zero across size classes. We further expect that many life history groups will deviate from EER. In particular, pioneer *fast* and *LL pioneers*—which are shade intolerant or recruit poorly in the understorey respectively—will deviate most strongly from the EER, while shade-tolerant *slow* species are the closest to the EER, at least at smaller sizes (Figure 1e).

Finally, we use a measure of light availability (Rüger et al., 2011)—based on tree size, position to neighbours, and light transmission through the canopy—to estimate individual tree light environment and test the hypothesis that pioneers increasingly gain a greater share of solar energy at larger sizes (Figure 1e,f). Because productivity is fuelled by resource use, we hypothesize there will be matching scaling slopes between productivity and total light interception with tree size, where total light interception is defined as the sum of intercepted light for all trees at a given stem size (Figure 1e). Thus, if whole-community productivity follows the EER—with a zero scaling slope—total light interception scaling will also have a zero slope with size. If confirmed, this would lend support for a resource-based corollary to the EER: a resource equivalence rule, in which all size classes have equal resource acquisition rates from the environment. Likewise, if particular life histories deviate from the EER, we expect their collective scaling of light interception will deviate by the same degree (Figure 1e).

To test predictions, we use data from a 50-ha primary forest tract of humid neotropical forest on BCI, Panama, where demographic data have been collected continuously for over three decades, and all life history strategies are near demographic equilibrium (Rüger et al., 2020). We exclude the perimeter of the forest where light penetration is influenced by non-plot forest we are unable to model, as well as a 2 ha portion of secondary growth, to yield a total of 42.84 ha of forest in our analysis. We use life history data and classification scheme of BCI trees from Rüger et al. (2018) to categorize woody plant life histories (1995 census). We categorize five life history strategies along fast–slow and stature–recruitment axes: *fast*, *slow*, *LL pioneer*, *SL recruiter*, as well as a *medium* classification that is intermediate to both axes (Figure S1). Following Rüger et al. (2011), we use a neighbourhood model to estimate light transmission and calculate individual and total light interception per size

class (see Section 2). We accommodate empirical deviation from a single power law fit at upper and lower tree size bounds by fitting piecewise power law distributions, that is, multiple power law fits with each segment connected. Unless otherwise noted, reported slopes represent the intermediate regression segment where most size variation occurs, ~3–50 cm stem diameter at breast height (dbh).

2 | MATERIALS AND METHODS

2.1 | Site and demographic data

We used long-term demographic data from a moist neotropical forest on BCI, Panama (9°9′ N, 79°51′ W). The forest at BCI is semi-deciduous, with a four-month dry season. Censuses of all free-standing woody stems ≥1 cm dbh, (measured 1.3 m from ground), at 0.1-cm resolution, excluding tree ferns and lianas, have been conducted on a 50-ha portion of the island at 5-year intervals since 1980; see Condit et al. (1998) for full description. We excluded perimeter and secondary forest in this plot to yield 43 ha for analysis. Growth analyses were based on the ~114,000 trees tagged both 1990 and 1995. We also included the ~18,000 new recruits from the 1995 census when fitting the abundance distributions for 1995, yielding a total of ~132,000 individuals.

2.2 | Life history classification and analysis

There is a long history of classifying trees into discrete life history or functional groups, such as pioneer/intermediate/shade-tolerant, or fast/slow (e.g. Hubbell et al., 1999; Reich, 2014; Ricklefs, 1977). We use a similar but more broadly defined trait-based classification based on Rüger et al. (2018). Rüger et al. analysed 282 species at BCI, using demographic data across four canopy layers plus seed and seedling data. Species scores in weighted PCA for growth, survival and recruitment rates. Following their classification scheme, we categorize trees as *fast*, *medium*, *slow*, *short-lived recruiter* (aka 'short-lived breeder') and *LL pioneer* (Figure S1). Specifically, both PCA axes were normalized by the absolute value of the 10th and 90th percentile values on that axis divided by two. All species within a radius of one from the origin were included in the *medium* group. The remaining species were divided into quadrants at a 45° angle from the PCA axes, resulting in five life history guilds.

Fast trees are characterized by fast growth in stem diameter, high mortality at all size stages, low wood density, high leaf N and P, and shade intolerance; *slow* trees are the opposite. On the *stature–recruitment* axis, *LL pioneers* have a large maximum size, poor sapling recruitment (despite abundant seedfall and seedlings), low mortality *and* fast growth. Conversely, *SL recruiters* are large shrubs and understorey trees with the opposite traits. *Medium* species are intermediate for both axes (Figure S1; Figure 3a). 2.1% of species at BCI are unclassified, that is, not classified in any life history category, including *medium*, but are included in plots and analyses of *All* species

(shown in black). *Fast* trees are short-lived and generally associated with tree gapfalls or disturbed areas that promote light penetration; thus, an alternative description for them could be short-lived pioneers. The reliance on light or disturbance for recruitment links *fast* species ('short-lived pioneers') and *LL pioneers* as 'pioneers' but their combined trait differences lead them to occupy very different places in trait space (Figure S1; Figure 3a), warranting treatment as distinct life history categories. Nonetheless, these categorical classifications represent different ends along a continuum rather than modal trait spaces. For this reason, we also regress mean tree PCA values of both dimensions against tree size and light intensity.

2.3 | Allometry from tree diameter measurements

At BCI, dbh is measured at 5-year census intervals. Reported regressions are based on the 1990–1995 census, but range bars from 1985 to 2010 censuses are shown in Figures 2 and 4, and in Figures S2–S4. We estimated the following measurements for all individual trees using allometric functions of dbh: tree height, crown area, crown depth, crown volume and above-ground biomass. We calculated diameter–height allometry and diameter–crown area allometry using parameter values generated from measurements taken on BCI (Cano et al., 2019). Cano et al. (2019) found that the generalized Michaelis–Menten function was the best fit for tree height, as it reaches an asymptote at high dbh values: $H = \frac{aD^b}{k + D^b}$, where D is dbh and a, b and k are constants. For crown area, a power law relationship fit best: $A = aD^b$, where D is dbh, A is crown area and a and b are constants. In both cases, we used species-specific coefficients provided from Cano et al. (2019) where possible, and the all-species coefficients for species not included in the study (9.1% of individuals).

Next, we estimated above-ground woody biomass (AGB) for each individual given individual dbh and height. The parameters of the allometry are taken from Chave et al. (2005) and were developed to apply across moist tropical forests: $AGB = 0.0509gD^2H$, where g is wood-specific gravity, D is dbh and H is tree height. This approach uses wood-specific gravity measurements at the genus or species level (measurements provided by K. C. Cushman, personal communication). After calculating AGB for each individual, we estimated AGB growth by taking the difference in AGB for a 5-year period: $\frac{\Delta AGB}{\Delta t}$. We converted this to annual mass growth rate G using the following equation: $G \equiv \frac{\Delta AGB}{\Delta t} = \frac{AGB_{t+\Delta t}}{AGB_t}\left(\frac{1}{\Delta t} - 1\right)$, where Δt is the census interval in days (roughly 5 years). We excluded individuals appearing for the first time in the tree census from the individual AGB analyses (14% of all individuals). We removed outliers where trees were recorded as gaining more than 20 cm dbh between two censuses or were entered into the census with >10 cm dbh following the first census, representing likely errors. This resulted in removing <300 individuals of 114,058. Above-ground woody productivity ('productivity', P) is the sum of G per cm dbh per ha (kg year^{-1} cm^{-1} ha^{-1}). Thus, it does not include the components of leaf growth, volatile organic carbon productivity, root productivity, discarded or consumed biomass, or reproductive organs.

Allometries for height, crown area and biomass were corrected for Jensen's inequality to eliminate biases in the height of curve resulting from log transformation (see 'Productivity Scaling Relationships' in Supporting Information S1). We took the correction factors for tree height and crown area from Cano et al. (2019).

2.4 | Model fitting

We used hierarchical Bayesian models to model the scaling of growth, abundance, richness, productivity and light interception for respective life histories. We evaluated fits with one, two and three segments, fitting piecewise log–log regressions to individual mass growth G, individual diameter growth, individual light interception and richness data and piecewise Pareto (power law) distributions to abundance data. Piecewise regression permits multiple power law fits to be fit and connected at multiple size ranges, which is useful if there are deviations from a single power law at different size classes. We used the widely applicable information criterion to select the optimal number of segments (Gelman et al., 2019). A single segment was best suited for mass growth and individual light interception and three-part segments for abundance following a Pareto distribution. To calculate productivity P, we took the product of the fitted values for abundance and individual mass growth across the range of sizes. For three-part regression fits in abundance and productivity, we report the middle regression fit, which covers most of the tree size range. Unlike abundance, which can be modelled as function of individual tree size distributions, richness is a collective attribute. Therefore, we fit regressions of richness to tree diameter or to abundance using mixed Bayesian linear model regression derived from size-binned values, with life history group as random effect. Finally, to model the scaling of mortality with tree size, we fit a non-linear logistic mixed-effects model with a J-curve functional form to capture the trend of mortality decreasing with increasing diameter for small trees but flatlining or increasing with increasing diameter at large sizes.

2.5 | Energy equivalence and productivity

Energy equivalence is based on the observation that a species' abundance per area A and organismal respiration R may scale inversely with organismal mass or size S: In particular, $R \propto S^\alpha$, $A \propto S^\beta$, $\alpha = -\beta$ and therefore $RA \propto S^0$. The EER has traditionally been measured indirectly by comparing regression fits of abundance scaling to literature references of metabolic scaling and assessing if they offset. This generally assumes a single power law fit across all sizes, but this may not be accurate (Muller-Landau, Condit, Chave, et al., 2006; Muller-Landau, Condit, Harms, et al., 2006). Originally, the EER applied to data in which one adult species had a single metabolic value and abundance, but has been since extended to species-agnostic size classes for taxa in the same trophic level with large size ranges, such as trees (e.g. West et al., 2009; see White et al., 2007 for discussion). The EER can therefore be written as $\overline{R}_i \propto S_i^\alpha$, $\overline{A}_i \propto S_i^\beta$ and $(\overline{R}_i\, \overline{A}_i) \propto S_i^0$, where i is stem size class and $\overline{R}_i$ and $\overline{A}_i$ are average values and $(\overline{R}_i\, \overline{A}_i)$ is the total respiration per size class. We follow this approach of focussing on differences between individuals at different sizes, rather than between species of different adult sizes. Although the EER has traditionally focussed on the scaling of individual respiration—which is challenging to measure at the whole-community scale—it has been extended to productivity, another metabolic process (West et al., 2009; Zhang et al., 2015). We follow this approach, focussing on the scaling of P with tree stem diameter (see Figure 2e).

We provide a better fit to data by using a three-piece regression for the scaling of abundance, which captures curvature while still retaining the ease of interpretability of linear models—for example, fitted coefficients represent the change in response variable per unit size. We then multiply fitted values of abundance scaling (regression line in Figure 2a) to fitted values of a one-segment model of the scaling of G (regression lines in Figure 4d) to calculate productivity scaling. A similar process is used to calculate total light interception scaling to test for solar energy equivalence. Tests of the EER are based on the intermediate segment regression fits that characterize most of the tree size range.

Alternatively, a more direct measure of productivity is to simply sum individual growth per stem size class i: $P_i = \sum_i^N G$, where N is the number of individuals. We use the latter approach to visualize productivity (Figure 2e) and total light interception $L_{Tot,i} = \sum_i^N L$, (plotted points in Figure 5a; Figure S6). See 'Binning and Plot Presentation' below for more discussion on binning.

2.6 | Quantifying light interception

To characterize the light environment for individual trees, we followed methods by Rüger et al. (2011). Specifically, we utilized published light estimates derived from annual censuses of vegetation density (http://richardcondit.org/data/canopy/bciCanopyReport.php). The presence/absence of vegetation was measured along a 5m grid across a 50-ha plot at BCI and at six height intervals: 0–2, 2–5, 5–10, 10–20, 20–30 and ≥30m. If vegetation was present, it was assumed to cast shade in the same manner as a 5m flat circle at the vertical midpoint of each height range. The proportion of open sky reaching a given tree was derived from a shade index based on irradiance and vegetation measurements taken at BCI, near the 50-ha plot area (Wirth et al., 2001). For a full description of the algorithm, see Rüger et al. (2011). Absolute irradiance reaching each tree was determined by multiplying the average overhead insolation at the latitude of BCI ($418\,W\,m^{-2}$ at $9°9'$ N) following North (1975) to the proportion of open sky for a tree to obtain the incoming light energy per area reaching the vertical projection area of the crown of each tree. To calculate light intensity, we divided this value by the crown area of each tree. 408 individuals (0.36%) lacked a modelled light value.

To calculate total light intercepted per stem size class, we used the same methods as for productivity: we used a one-segment regression model of intercepted light and stem diameter and a

three-segment regression model for abundance by dbh for each life history. We multiplied the fitted values of individual light received and abundance to yield the total light scaling relationship.

2.7 | Binning and plot presentation

The wealth of data at long-term monitoring sites is invaluable but can present challenges for presentation. First, it is difficult to visually assess variation between life history strategies when there are >100,000 data points overlapping on a plot. Second, non-linearities are also obscured by such an abundance of overlapping data. Finally, despite drawing from the same large data pool, collective attributes like abundance and productivity do not have individual data values for presentation. For these reasons, we show piecewise regression fits and 95% credible interval (CI) bands without raw data, as well as binned mean or summed quantities per stem size class to indicate empirical central tendency patterns, including non-linearities. Thus, empirical deviation from a regression fit—such as curvilinearity near the upper or lower bounds of the data—is apparent to the viewer. Using binned data, we can plot and compare trees from different life histories. Error and parameter values associated with regression fits are provided in Table 1 and Supporting Information S2.

To bin summed data, we follow White et al. (2008) by plotting summed abundance, productivity and light interception that is measured over stem diameter or light intensity bin increments in logarithmic space and then divided by the bin range to show arithmetic mean values per unit cm stem diameter. Note all reported values are per unit plot area (ha^{-1}), except richness. Richness is per plot (42.84 ha) rather than ha, since richness scales allometrically with plot area. All plotted points have a minimum of 20 individuals per bin.

2.8 | Code and data availability

All models were coded in the Stan language. In all cases, we used Hamiltonian Monte Carlo to sample from the posterior distribution, with three chains, 5000 warm-up samples per chain that we discarded, and 1000 post-warm-up samples per chain that we retained. We assessed convergence of posterior distributions by visually examining trace plots and by ensuring $\hat{R} < 1.1$ for all parameters (Gelman & Rubin, 1992). Data and R code required to reproduce our analysis are archived at Zenodo at https://doi.org/10.5281/ze-nodo.10407633. BCI survey data are publicly available through the Smithsonian Institution (https://repository.si.edu/handle/10088/20925). See Supporting Information for complete description.

3 | RESULTS

We measured the scaling of abundance, richness, above-ground woody productivity and light interception in five life history strategies to test four hypotheses: (i) that pioneer life histories (*fast* and *LL pioneers*) increase in relative frequency to *slow* species at larger sizes, (ii) that life history richness follows a power law with abundance, (iii) that life histories converge or diverge predictably towards energy equivalence and (iv) that light interception tracks the scaling of above-ground woody productivity.
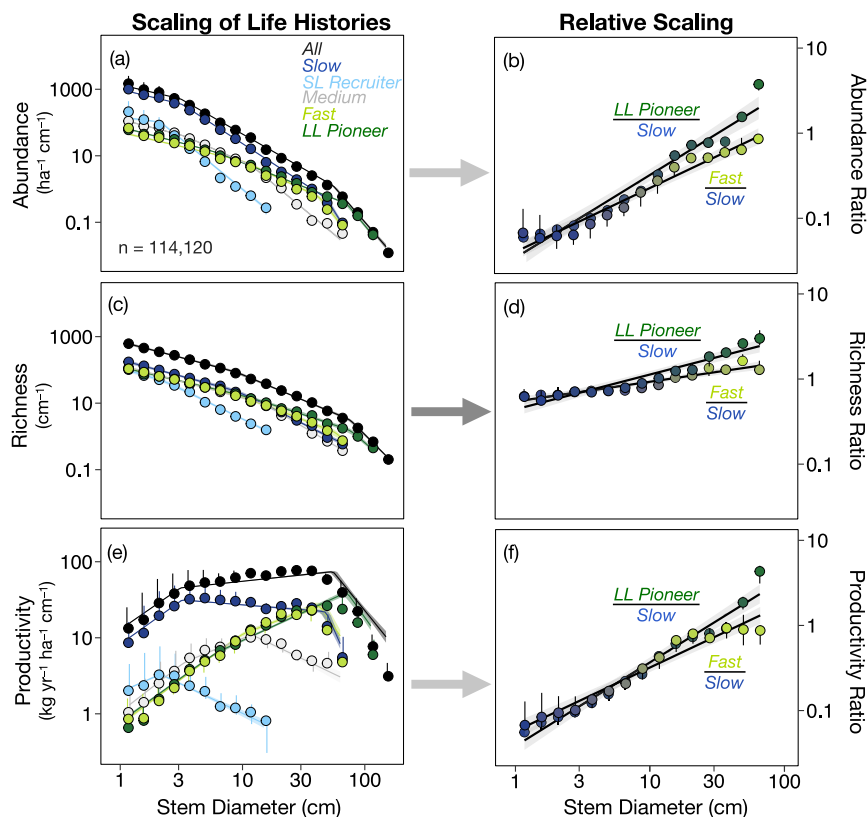

FIGURE 2 The scaling of life history frequency in trees. Scaling piecewise regressions of abundance per area (a), richness per plot (c) and above-ground woody productivity (e) are shown for each life history group, with 95% credible bands (shaded). Relative shifts in canopy-forming trees are shown on the right by regressing the ratio of *fast* or *LL pioneer* values to *slow* against stem diameter (b, d, f). Each point represents a minimum of 20 individuals per life history group. Vertical range bars for points span 20 years of sampling; some ranges are too small to be visible, but see Figures S2–S5. Abundance and richness values are from a 1995 census and 1990–1995 for productivity. Panels a–c and b–d are plotted on the same scale for comparison, showing that abundance changes more steeply than richness with tree size. LL, long-lived.

Demographic patterns of life history scaling support our first hypothesis. At the smallest stem size classes, *slow* species are by far the most abundant saplings in the understorey, with small, *SL recruiters* a distant second (Figure 2a). *Slow* trees then decline steadily in abundance from ~70% at 3 cm dbh to ~50% at 10 cm dbh, and finally <8% at 100 cm dbh. This decline is offset by a rapid increase in the relative abundance of *fast* and *LL pioneers*, which achieve numerical parity or superiority in the upper canopy. The demographic shift reflects differences in abundance scaling with size: *slow* trees decline in abundance with size at a faster rate than *LL pioneer* and *fast* trees (Table 1; $slope_{slow} = -2.40$, 95% quantile CI = −2.38, −2.42; $slope_{fast} = -1.71$, CI: −1.60, −1.82; $slope_{LLpioneer} = -1.45$, CI: −1.40, −1.50). This difference in slopes leads to an ~order of magnitude decline in the relative abundance of *slow* species towards the canopy, where they are equalled by *fast* species and surpassed by *LL pioneers* (Figure 2a,b). At smaller size classes, hyperabundant *slow* trees effectively drive whole community scaling patterns of abundance, but towards the canopy they are no more common than *fast* and *LL pioneer* trees. Consistent with their small maximum sizes, the relative abundance of *SL recruiter* shrubs and understorey trees declines rapidly at larger size classes, with a steep slope of −3.02 (CI: −3.01, −2.94; Figure 2a; Table 1). Similar to scaling shifts in relative abundance, the mean life history PCA loadings for all trees change directionally with size and light availability, from values closer to *slow* and *SL recruiter* loadings at small sizes and low light towards *fast* to *LL pioneers* loading values at larger stem diameters and light levels (Figure 3).

Supporting our second prediction, the scaling patterns of absolute and relative richness patterns mirror power law shifts in abundance, but with shallower slopes that are >−2 (Figure 2c vs. 2a; Table 1). Likewise, regressing richness against abundance on a log–log plot reveals a slope <1 for all life history strategies (Figure 4a; all slope 95% CI's are <1, see Supporting Information S2), indicating that richness increases sublinearly with abundance. Like abundance, richness per unit cm is the highest at small sizes, but declines with stem diameter following a power law. Interestingly, despite notable non-linearities in abundance and richness scaling on their own (Figure 2a,c), when richness is

regressed against abundance the results are almost perfectly linear on a log plot (Figure 4a). The slopes and intercepts of the regression fits of richness against abundance across life histories are largely similar, but show some divergences (*LL pioneer* slope is 0.75 (CI: 0.72–0.77) versus 0.59 for *slow* trees (CI: 0.56–0.63). In particular, *slow* species have the fewest species per individual in the understorey while *fast*, *LL pioneer and medium* have the highest species per individual at small size classes (Figure 4a). However, all life history strategies converge in the canopy where abundance is the lowest, maintaining ~one species per five individuals. Note that abundances and richness reflect size-binning shown in Figure 2a,c, in which the highest abundances correspond to the smallest size classes and vice versa.

Above-ground woody productivity scaling patterns help clarify the role of tree size in the metabolic production of carbon. Reflecting their higher abundances on the forest floor, *slow* trees produce nearly an order of magnitude higher productivity at the smallest size class, but productivity declines to parity with *fast* and *LL pioneers* at ~30 cm dbh (Figure 2e,f). As predicted, *slow* trees are the closest to an energy equivalence of productivity (slope = 0), with a slight decline in woody production towards the canopy (slope of −0.13; CI: −0.16, −0.12; Table 1). In *medium* and pioneer life history strategies (*fast* and *LL pioneers*), there is a much stronger and opposing deviation from equivalence, with steep increases in absolute and relative productivity in *fast* and *LL pioneers* towards the canopy (Figure 2e,f; $slope_{Fast} = 0.62$, CI: 0.49, 0.73; $slope_{LLpioneer} = 0.75$, CI: 0.70, 0.80; Table 1). At the whole-community scale, *all* trees are collectively close to EER (Figure 2e, slope = 0.18, CI: 0.16–0.19). This reflects the outsized contribution of *slow* species near energy equivalence, which comprise only 22% of species but over 65% of individuals (Table 1).

To better understand some of the drivers of life history scaling, we also explored demographic components of community abundance and productivity. Demographic size distributions, such as abundance scaling, are a function of diameter growth and recruitment into new stem size classes, which is counterbalanced by mortality and growth out of a size class (Condit et al., 1998; Lima et al., 2016). Since *fast* trees are, in part, defined by rapid diameter
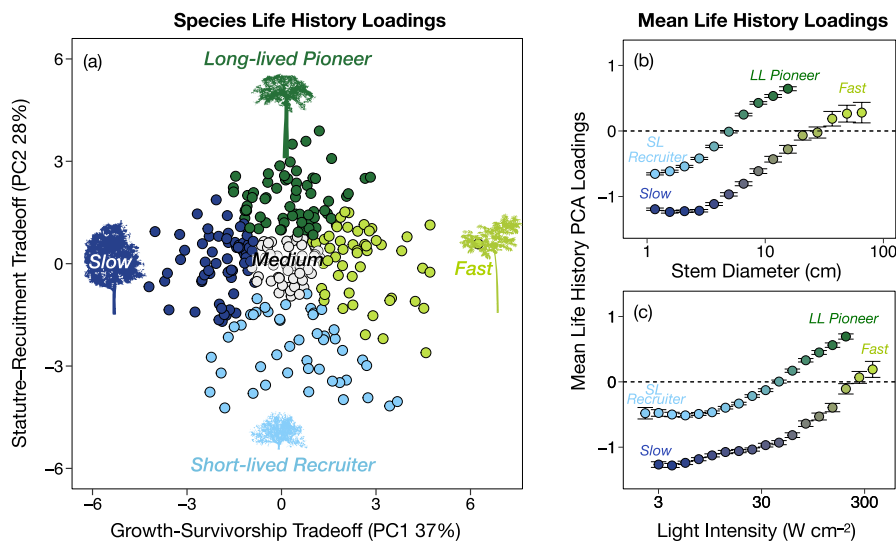

FIGURE 3 Changes in life history loadings with size and light intensity. (a) Principal component analysis (PCA) loadings for each species at the Barro Colorado Island study site; data from Rüger et al. (2018). Mean PCA loadings with 95% credible intervals for all individuals with respect to (b) tree size (diameter at breast height) and (c) light intensity or irradiance (rate per unit crown area).
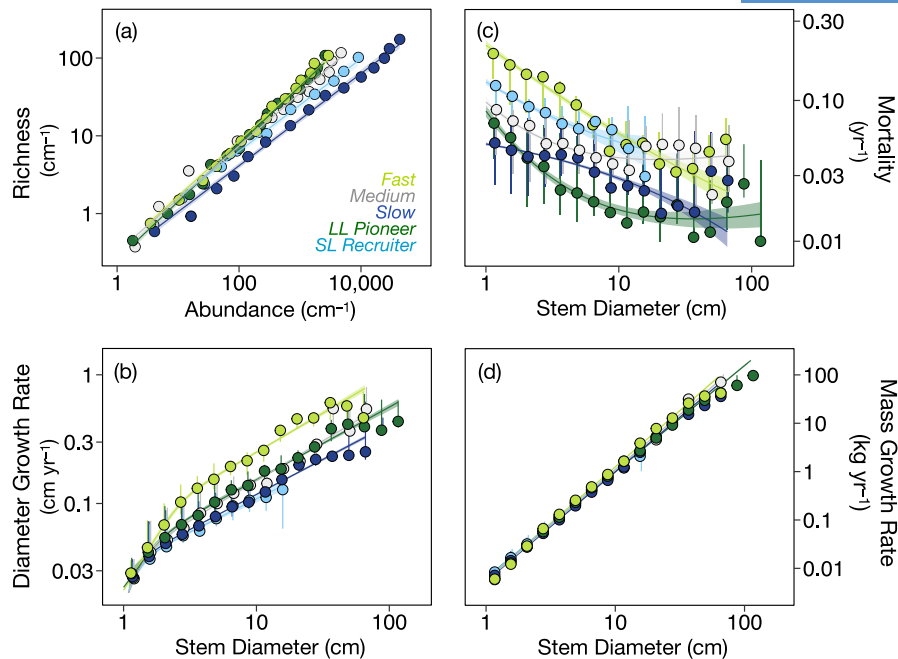
FIGURE 4 Demographic components of life history scaling. In (a), richness is an allometric function of abundance, with slopes <1 for all groups (Supporting Information S2). Demographic components of abundance scaling include stem diameter growth rate (b) and mortality (c); components of productivity are abundance and individual mass growth rate in (d). Note that while life history strategies are categorized, in part, by differences in diameter growth, rates converge at the smallest sizes in (b), and mass growth rates are similar at all sizes in (d). All regression fits are plotted with shaded 95% credible bands. Vertical bars are ranges from other census years, but are not always large enough to be visible (see Figures S4 and S5).

growth and high mortality, it follows that *fast* show the greatest diameter growth rates (cm year^{-1}) for a given size (Figure 4b). However, these differences are size dependent. Diameter growth for all species are approximately equivalent at the smallest stem size classes but diverge sharply with size, reflecting differences in slope (Supporting Information S1). This may reflect a higher sensitivity of *fast* species to light, which increases towards the canopy. Again, patterns of mortality broadly fit expectations, but there are shifts in ranking with size: *slow* trees have the lowest mortality and *fast* trees the highest at small sizes, but *LL pioneers* have the lowest mortality above the sapling stage (>3 cm dbh), while *fast* trees converge towards other life histories when large (Figure 4c). Thus, the higher abundance of *LL pioneers* and *fast* species in the upper canopy is consistent with their combination of low mortality plus fast stem diameter growth for *LL pioneers*, and fast diameter growth and declining mortality with size for *fast* species.

Above-ground woody productivity is the product of abundance and individual woody mass growth *G*. In contrast to diameter growth (Figure 4b), it is striking how similar individual mass growth is for all life history strategies, both in terms of absolute values and slopes (Figure 4d; Supporting Information S2). *Fast* trees show modestly steeper slopes for mass growth, but overall there is little difference between groups. Thus, increases in productivity in *fast* and *LL pioneer* species compared to *slow* are driven by increases in relative abundance with size, not differences in mass growth rates. These scaling patterns are stable across census years (Figures S2–S5).
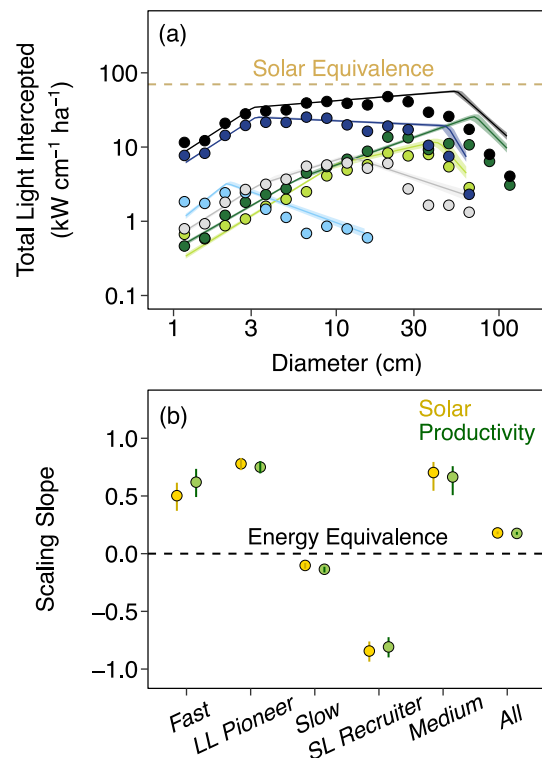

FIGURE 5 Light interception scaling and energy equivalence. (a) Scaling patterns of total light interception are similar to productivity (Figure 2e); slope comparisons of intermediate regression fits are shown in (b), with 95% CI bars. Credible intervals overlap for all paired groups (b).

TABLE 1 Scaling exponents for life history strategies at Barro Colorado Island. Results support life history predictions in Figure 1. Note the similarity in slopes for productivity and total light interception, supporting predictions in Figure 1e. Slopes for abundance, productivity and light interception are from the intermediate portion of three-part, piecewise Pareto fits: ~3–50 cm dbh; 95% credible intervals are shown in parentheses. 2809 individuals (2.1% of total) were unclassified and are included in statistics for *All*. N and Spp. represent the number of individuals and species, respectively, over two sampling periods (1990 and 1995). Richness, Spp. and N trees are per plot (43 ha); all other values are per ha.

Life history	Abundance (ha^{-1} cm^{-1})	Richness (cm^{-1})	Above woody productivity (kg year^{-1} ha^{-1} cm^{-1})	Total light interception (W ha^{-1} cm^{-1})	Spp.	N trees
Fast	−1.71 (−1.84, −1.60)	−0.557 (−1.00, −3.07)	0.620 (0.491, 0.735)	0.504 (0.371, 0.615)	52	8898
LL Pioneer	−1.45 (−1.50, −1.40)	−0.394 (−0.834, −0.177)	0.751 (0.695, 0.803)	0.780 (0.724, 0.830)	65	11,136
Slow	−2.40 (−2.42, −2.38)	−0.853 (−1.02, −0.694)	−0.134 (−0.163, −0.113	−0.101 (−0.130, 0.081)	64	86,864
SL recruiter	−3.02 (−3.10, −2.94)	−0.721 (−0.983, −0.334)	−0.807 (−0.899, −0.724)	−0.843 (−0.936, −0.761)	44	10,456
Medium	−1.63 (−1.79, −1.54)	−1.177 (−1.37, −0.948)	0.665 (0.507, 0.758)	0.704 (0.545, 0.795)	52	12,817
All	−2.09 (−2.10, −2.08)	−0.577 (−0.705, −0.443)	0.176 (0.164, 0.189)	0.181 (0.168, 0.192)	293	132,982

3.1 | Light interception and resource use equivalence

Finally, we reasoned that if resources fuelled productivity, the size-dependence of light capture should match the size-dependence of productivity. Supporting these predictions, we do not find significant differences in the scaling slopes of productivity and light capture for any life history strategy, with CI intervals overlapping for all life histories (Figure 5; Figure S6; Table 1; Supporting Information S2), and the scaling of total light capture largely mirrors patterns of productivity (Figure 2e). This pattern extends to an approximate size invariance in intercepted light for *all* individuals at the community scale. Thus, we offer support for a resource use equivalence with size that matches a productivity energy equivalence. The tracking of light interception with productivity also provides an explicit metric of changing resource competition with size. Because *LL pioneers* and *fast* species are more abundant and productive at larger sizes (Figure 2), they also increase their share of limited solar resources in a closed canopy forest (Figure 5), consistent with predictions (Figure 1e,f).

4 | DISCUSSION

Tree size and life history variation are major drivers of forest structure and dynamics. We show that they interact following allometric power laws at BCI such that the proportion of species in a given life history group shifts systematically with tree size. Despite being outnumbered more than 10:1 in the understorey, *fast* and *LL pioneer* species rapidly increase their abundance, productivity and richness relative to shade-tolerant *slow* species until reaching or exceeding parity in the canopy. Indeed, despite representing only 15% of individuals, *fast* and *LL pioneer* species together produce as much annual biomass as *slow* species that are more than four times as abundant.

The high abundance of *slow* species in the understorey may reflect a 'sit and wait' strategy of shade-tolerant trees that can

spend decades in a suppressed state of growth while waiting for sufficient light conditions to develop. Conversely, the proportional increase in pioneer trees towards the canopy is consistent with their elevated growth rates and low mortality, in the case of *LL pioneers*, or fast growth and declining mortality with size in the case of *fast* species. By definition, *fast* trees grow quickly in stem diameter but, intriguingly, have roughly the same aboveground woody growth rate in biomass as all other life histories at a given size (Figure 4b, Rüger et al., 2012). Thus, higher diameter growth in pioneers is likely a function of lower wood density, rather than elevated carbon fixation rates at the whole tree level. In addition to wood density, pioneer and shade-tolerant trees also differ in other aspects of construction, including total leaf area and per leaf photosynthetic rates (Rüger et al., 2018; Valladares & Niinemets, 2008). The convergence of woody growth in biomass across life history strategies points towards general trade-offs that strongly constrain individual tree productivity at given size. For instance, *fast* trees—with higher foliar N, P and leaf photosynthetic rates—are also the most shade limited (Iida et al., 2011). To avoid self-shading, they have lower total leaf area, limiting whole-tree productivity to approximately the same rates as *slow* species.

4.1 | Energy use with tree size

A general pattern in ecological communities is that large organisms are rare. Indeed, the number of individuals per area often decline with organismal size following a power law. The magnitude of this scaling relationship is counterbalanced by a power law increase in per capita respiration or growth rate with individual size. When the magnitudes offset, a system is said to follow the EER: all size classes flux equal amounts of metabolic energy. The EER has been widely documented in forests and other autotrophic systems and, given its ubiquity, has been argued to structure forests (Deng et al., 2008; Perkins et al., 2019; West et al., 2009). At BCI, we examined patterns of above-ground woody productivity to assess whether the EER occurs not only at the whole-community

level but also across life history strategies. Indeed, at the whole-community level, productivity is near energy equivalence, with similar levels of productivity between stem size class from 3 to 50 cm dbh. Across life history strategies, however, only *slow* species were near energy equivalence, declining modestly in energy use at large stem size classes. In contrast, *LL pioneers* and *fast* species increased in total productivity over an order of magnitude with size, as they disproportionately increased in abundance towards the canopy. Thus, even in systems constrained by the EER, functional groups within may strongly diverge.

All trees use light, water and nutrients to capture carbon and produce biomass. For these reasons, we predicted the scaling of productivity across life history strategies to broadly match the scaling of resource use. In principle, however, the scaling of total light interception could diverge from productivity scaling if light use efficiency varied greatly. For instance, canopy trees experiencing over-saturated light levels may not be able to convert intercepted light into carbon as efficiently as understorey trees. Nonetheless, we expected that the scaling of productivity and light interception to be similar for two reasons. First, there are adaptive and biophysical constraints on how much variation in light use efficiency is possible in a forest. Second, and more importantly, much of the scaling of productivity and total light interception is a function of abundance, which varies orders of magnitude more than light use efficiency with size. Supporting our hypothesis, we found a general congruence between variables: the scaling of total light interception and productivity were nearly identical for each life history group and at the whole-community scale.

The symmetry in productivity and total light capture is intriguing given the fact that incoming light flux is, on average, two orders of magnitude greater at the top of the canopy than in the understorey. The implication is that the patterns of mortality, abundance and the spatial arrangement of trees from efficient gap-filling (Purves et al., 2008) are such that each stem size class intercepts similar amounts of light. Indeed, this pattern of light interception has been observed in aerial Lidar analyses at the whole forest community scale (Stark et al., 2012), though how functional groups within the forests behaved has been unclear until now. Overall, our results point towards an important corollary of the EER: the resource equivalence rule. In systems following the EER, resource use rates across size classes are expected to be approximately equivalent.

Deviation from the EER across life history strategies can offer insights into how resource competition changes with size and other traits. At BCI, pioneer life histories are not only more relatively abundant at large sizes but are also more competitive, increasing their proportional share of resources by an order of magnitude from saplings to the canopy. Further, the share of solar resources gained by fast-growing *fast* and *LL pioneer* species—with generally higher leaf nitrogen, phosphorus, carbon fixation and respiration rates (Rüger et al., 2018; Valladares & Niinemets, 2008)—increases with average light availability. That is, trees with higher leaf metabolism tend to predominate in high-light environments, and vice versa.

These *within-community* findings complement *cross-community* research demonstrating that faster growing/metabolizing species tend to be more common or competitively successful in high resource habitats for plants (Grime, 1988; Reich, 2014) and animal communities (Grady et al., 2019). Faster metabolism generally has fitness benefits—faster growth, faster reproduction and faster movement—but at the cost of higher resource requirements. Such a mapping of metabolic traits with resource availability may be a widespread feature of ecological systems.

4.2 | Life history trade-offs and diversity

Coexistence theory stipulates that coexistence is possible if total intra-specific competition across life stages exceeds the total effects of inter-specific competition across life stages (Bassar et al., 2017; Chesson, 2000), leading to 'stabilizing' niche differentiation (sensu Chesson, 2000). For instance, coexistence can occur in two populations if each is a better competitor at different sizes. Indeed, Baraloto et al. (2005) observed patterns of reversal in survival and relative growth rank in some tropical seedlings that were consistent with ontogenetic performance trade-offs. Relative abundance is a more integrated measure of fitness, however, than either survival or growth rate in isolation. At BCI, we observe a strong shift in the relative abundance with size, with all groups converging on parity or showing rank reversal in abundance, richness, or productivity at the canopy, despite an order of magnitude head start in abundance among *slow* saplings (Figure 2). Similarly, mean life history PCA scores shift from one side of the continuum to the other as tree size and light intensity increase (Figure 3). These scaling shifts in life history frequency have parallels to niche partitioning with light, with *fast* and *LL pioneers* in the high-light canopy niche, and *slow* species occupying the low-light understorey niche.

Alternatively, ontogenetic trade-offs across life histories may represent an 'equalizing' or neutral force that promotes coexistence by reducing whole-organismal fitness differences (Chesson, 2000). That is, despite important functional differences, pioneer and *slow* species may be competitively equivalent when examined over the full size-range of ontogeny. There are limits, of course: if fitness differences are strong enough at any size, coexistence is unstable and exclusion will occur (Bassar et al., 2017). For example, if pioneer species do not receive sufficient rates of disturbance, they may be out-competed by the sapling stage before ever reaching the canopy. Given that life history trade-offs with size can support diversity in two independent ways, disentangling whether observed life history scaling is more consistent with stabilizing or equalizing processes deserves more attention.

Another link between life history variation and diversity is more general. We observed all life history strategies became more speciose at higher densities, following remarkably regular power laws (Figure 4a). This positive abundance–richness pattern has parallels to the 'more individuals hypothesis' of diversity, in which more productive communities have higher richness because they support more

individuals (Srivastava & Lawton, 1998). It is also consistent with the long recognized species–area relationship in which species richness is an allometric function of land area (Connor & McCoy, 1979). In particular, if abundance is proportional to area, and richness is an allometric function of area, then it follows that richness should be an allometric function of abundance. What is different in this study, however, is that we observe this pattern *within* a community in a fixed area, rather than *across* communities. Further, the similarity in abundance–richness relationships for all life history strategies is indicative of deep functional convergences in tree species despite divergent traits. This lends support to an important mechanism of diversity maintenance: Hubbell's argument of 'functional equivalence' or neutrality between coexisting species that limits competitive exclusion (Hubbell, 2005).

5 | SYNTHESIS

We show that the proportion of individuals and resource use from a life history group changes systematically with size, consistent with ontogenetic trade-offs. In particular, fast-growing pioneer trees increase proportionally in abundance at larger size classes towards the high-light canopy, while shade-tolerant trees with a *slow* life history decline. Along with this shift in abundance, pioneer trees also increase their share of richness, productivity, light interception and other resources towards the canopy. Trade-offs in competitive fortunes over ontogeny may represent an important mechanism for maintaining diversity in forests and other systems. Moving forward, quantifying links between organismal size, trait frequency and resource share will provide deeper insights into the adaptive significance of size and life history strategy.

AUTHOR CONTRIBUTIONS

John M. Grady conceived the study and developed theory. John M. Grady and Quentin D. Read wrote the paper and performed analyses. John M. Grady, Quentin D. Read, Nadja Rüger, Sydne Record and Brian J. Enquist designed the approach. Nadja Rüger and Stephen P. Hubbell contributed data. John M. Grady, Quentin D. Read, Brian J. Enquist, Nadja Rüger, Sean T. Michaletz and Anthony I. Dell discussed the results and edited the manuscript.

CONFLICT OF INTEREST STATEMENT

We have no conflict of interest to report.

PEER REVIEW

The peer review history for this article is available at https://www.webofscience.com/api/gateway/wos/peer-review/10.1111/1365-2745.14245.

DATA AVAILABILITY STATEMENT

Data, analyses and results are available at Zenodo: https://doi.org/10.5281/zenodo.10407633 (Read and Grady, 2023).

ORCID

John M. Grady https://orcid.org/0000-0001-6444-3300
Quentin D. Read https://orcid.org/0000-0003-4315-5582
Sydne Record https://orcid.org/0000-0001-7293-2155
Nadja Rüger https://orcid.org/0000-0003-2371-4172
Phoebe L. Zarnetske https://orcid.org/0000-0001-6257-6951
Stephen P. Hubbell https://orcid.org/0000-0003-2797-3411
Sean T. Michaletz https://orcid.org/0000-0003-2158-6525
Brian J. Enquist https://orcid.org/0000-0002-6124-7096

REFERENCES

Álvarez-Yépiz, J. C., Búrquez, A., Martínez-Yrízar, A., Teece, M., Yépez, E. A., & Dovciak, M. (2017). Resource partitioning by evergreen and deciduous species in a tropical dry forest. *Oecologia*, *183*, 607–618.

Baraloto, C., Goldberg, D. E., & Bonal, D. (2005). Performance trade-offs among tropical tree seedlings in contrasting microhabitats. *Ecology*, *86*, 2461–2472.

Bassar, R. D., Travis, J., & Coulson, T. (2017). Predicting coexistence in species with continuous ontogenetic niche shifts and competitive asymmetry. *Ecology*, *98*, 2823–2836.

Bennett, A. C., McDowell, N. G., Allen, C. D., & Anderson-Teixeira, K. J. (2015). Larger trees suffer most during drought in forests worldwide. *Nature Plants*, *1*, 15139.

Bohlman, S., & O'Brien, S. (2006). Allometry, adult stature, and regeneration requirement of 65 tree species on Barro Colorado Island, Panama. *Journal of Tropical Ecology*, *22*, 123–136.

Brokaw, N., & Busing, R. T. (2000). Niche versus chance and tree diversity in forest gaps. *Trends in Ecology & Evolution*, *15*, 183–188.

Busing, R. T., & White, P. S. (1997). Species diversity and small-scale disturbance in an old-growth temperate forest: A consideration of gap partitioning concepts. *Oikos*, *78*, 562–568.

Canham, C. D., Papaik, M. J., & Latty, E. F. (2001). Interspecific variation in susceptibility to windthrow as a function of tree size and storm

severity for northern temperate tree species. *Canadian Journal of Forest Research*, *31*, 1–10.

Cano, I. M., Muller-Landau, H. C., Wright, S. J., Bohlman, S. A., & Pacala, S. W. (2019). Tropical tree height and crown allometries for the Barro Colorado Nature Monument, Panama: A comparison of alternative hierarchical models incorporating interspecific variation in relation to life history traits. *Biogeosciences*, *16*, 847–862.

Chave, J., Andalo, C., Brown, S., Cairns, M. A., Chambers, J., Eamus, D., Fölster, H., Fromard, F., Higuchi, N., & Kira, T. (2005). Tree allometry and improved estimation of carbon stocks and balance in tropical forests. *Oecologia*, *145*, 87–99.

Chesson, P. (2000). Mechanisms of maintenance of species diversity. *Annual Review of Ecology and Systematics*, *31*, 343–366.

Condit, R. (1998). *Tropical forest census plots: Methods and results from Barro Colorado Island, Panama and a comparison with other plots.* Springer Science & Business Media.

Condit, R., Ashton, P., Bunyavejchewin, S., Dattaraja, H. S., Davies, S., Esufali, S., Ewango, C., Foster, R., Gunatilleke, I. A. U. N., Gunatilleke, C. V. S., Hall, P., Harms, K. E., Hart, T., Hernandez, C., Hubbell, S., Itoh, A., Kiratiprayoon, S., LaFrankie, J., de Lao, S. L., … Zillio, T. (2006). The importance of demographic niches to tree diversity. *Science*, *313*, 98–101. https://doi.org/10.1126/science.1124712

Condit, R., Sukumar, R., Hubbell, S. P., & Foster, R. B. (1998). Predicting population trends from size distributions: A direct test in a tropical tree community. *The American Naturalist*, *152*, 495–509.

Connor, E. F., & McCoy, E. D. (1979). The statistics and biology of the species-area relationship. *The American Naturalist*, *113*, 791–833.

Damuth, J. D. (1998). Common rules for animals and plants. *Nature*, *395*, 115–116.

Deng, J.-M., Li, T., Wang, G.-X., Liu, J., Yu, Z.-L., Zhao, C.-M., Ji, M.-F., Zhang, Q., & Liu, J.-Q. (2008). Trade-offs between the metabolic rate and population density of plants. *PLoS One*, *3*, e1799.

Gelman, A., Goodrich, B., Gabry, J., & Vehtari, A. (2019). R-squared for Bayesian regression models. *The American Statistician*, *73*, 307–309.

Gelman, A., & Rubin, D. B. (1992). Inference from iterative simulation using multiple sequences (with discussion). *Statistical Science*, *7*, 457–511.

Gilbert, G. S., Reynolds, D. R., & Bethancourt, A. (2007). The patchiness of epifoliar fungi in tropical forests: Host range, host abundance, and environment. *Ecology*, *88*, 575–581.

Gora, E. M., Muller-Landau, H. C., Burchfield, J. C., Bitzer, P. M., Hubbell, S. P., & Yanoviak, S. P. (2020). A mechanistic and empirically supported lightning risk model for forest trees. *Journal of Ecology*, *108*, 1956–1966.

Grady, J. M., Maitner, B. S., Winter, A. S., Kaschner, K., Tittensor, D. P., Record, S., Smith, F. A., Wilson, A. M., Dell, A. I., & Zarnetske, P. L. (2019). Metabolic asymmetry and the global diversity of marine predators. *Science*, *363*, eaat4220.

Grime, J. P. (1988). The CSR model of primary plant strategies—Origins, implications and tests. In L. D. Gottlieb & S. K. Jain (Eds.), *Plant evolutionary biology* (pp. 371–393). Springer.

Hubau, W., De Mil, T., Van den Bulcke, J., Phillips, O. L., Angoboy Ilondea, B., Van Acker, J., Sullivan, M. J., Nsenga, L., Toirambe, B., & Couralet, C. (2019). The persistence of carbon in the African forest understory. *Nature Plants*, *5*, 133–140.

Hubbell, S. P. (2005). Neutral theory in community ecology and the hypothesis of functional equivalence. *Functional Ecology*, *19*, 166–172.

Hubbell, S. P., Foster, R. B., O'Brien, S. T., Harms, K., Condit, R., Wechsler, B., Wright, S. J., & De Lao, S. L. (1999). Light-gap disturbances, recruitment limitation, and tree diversity in a neotropical forest. *Science*, *283*, 554–557.

Iida, Y., Kohyama, T. S., Kubo, T., Kassim, A. R., Poorter, L., Sterck, F., & Potts, M. D. (2011). Tree architecture and life-history strategies across 200 co-occurring tropical tree species. *Functional Ecology*, *25*, 1260–1268.

Kitajima, K., & Poorter, L. (2008). Functional basis for resource niche partitioning by tropical trees. *Tropical Forest Community Ecology*, *1936*, 160–181.

Kohyama, T. S., Potts, M. D., Kohyama, T. I., Kassim, A. R., & Ashton, P. S. (2015). Demographic properties shape tree size distribution in a Malaysian rain forest. *The American Naturalist*, *185*, 367–379.

Kohyama, T. S., & Takada, T. (2012). One-sided competition for light promotes coexistence of forest trees that share the same adult height. *Journal of Ecology*, *100*, 1501–1511.

Lieberman, M., Lieberman, D., Peralta, R., & Hartshorn, G. S. (1995). Canopy closure and the distribution of tropical forest tree species at La Selva, Costa Rica. *Journal of Tropical Ecology*, *11*, 161–177.

Lima, R. A., Muller-Landau, H. C., Prado, P. I., & Condit, R. (2016). How do size distributions relate to concurrently measured demographic rates? Evidence from over 150 tree species in Panama. *Journal of Tropical Ecology*, *32*, 179–192.

Lutz, J. A., Furniss, T. J., Johnson, D. J., Davies, S. J., Allen, D., Alonso, A., Anderson-Teixeira, K. J., Andrade, A., Baltzer, J., Becker, K. M. L., Blomdahl, E. M., Bourg, N. A., Bunyavejchewin, S., Burslem, D. F. R. P., Cansler, C. A., Cao, K., Cao, M., Cárdenas, D., Chang, L.-W., … Zimmerman, J. K. (2018). Global importance of large-diameter trees. *Global Ecology and Biogeography*, *27*, 849–864. https://doi.org/10.1111/geb.12747

Madigosky, S. R. (2004). Tropical microclimatic considerations. In M. D. Lowman & H. B. Rinker (Eds.), *Forest canopies* (pp. 24–48). Eleesevier.

McClain, C. R. (2004). Connecting species richness, abundance and body size in deep-sea gastropods. *Global Ecology and Biogeography*, *13*, 327–334.

Molino, J.-F., & Sabatier, D. (2001). Tree diversity in tropical rain forests: A validation of the intermediate disturbance hypothesis. *Science*, *294*, 1702–1704.

Muller-Landau, H., Condit, R., Chave, J., Thomas, S., Bohlman, S., Bunyavejchewin, S., Davies, S., Foster, R., Gunatilleke, S., & Gunatilleke, N. (2006). Testing metabolic ecology theory for allometric scaling of tree size, growth and mortality in tropical forests. *Ecology Letters*, *9*, 575–588.

Muller-Landau, H. C., Condit, R. S., Harms, K. E., Marks, C. O., Thomas, S. C., Bunyavejchewin, S., Chuyong, G., Co, L., Davies, S., & Foster, R. (2006). Comparing tropical forest tree size distributions with the predictions of metabolic ecology and equilibrium models. *Ecology Letters*, *9*, 589–602.

Niklas, K. (2004). Plant allometry: Is there a grand unifying theory? *Biological Reviews*, *79*, 871–889.

Niklas, K. J. (1994). *Plant allometry: The scaling of form and process.* University of Chicago Press.

North, G. R. (1975). Analytical solution to a simple climate model with diffusive heat transport. *Journal of the Atmospheric Sciences*, *32*, 1301–1307.

Perkins, D. M., Perna, A., Adrian, R., Cermeño, P., Gaedke, U., Huete-Ortega, M., White, E. P., & Yvon-Durocher, G. (2019). Energetic equivalence underpins the size structure of tree and phytoplankton communities. *Nature Communications*, *10*, 255.

Poorter, L., Bongers, L., & Bongers, F. (2006). Architecture of 54 moist-forest tree species: Traits, trade-offs, and functional groups. *Ecology*, *87*, 1289–1301.

Purves, D. W., Lichstein, J. W., Strigul, N., & Pacala, S. W. (2008). Predicting and understanding forest dynamics using a simple tractable model. *Proceedings of the National Academy of Sciences of the United States of America*, *105*, 17018–17022.

Read, Q. D., & Grady, J. M. (2023). qdread/forestscalingworkflow. v3.1. *Zenodo.* https://doi.org/10.5281/zenodo.10407633

Reich, P. B. (2014). The world-wide 'fast–slow' plant economics spectrum: A traits manifesto. *Journal of Ecology*, *102*, 275–301.

Ricklefs, R. E. (1977). Environmental heterogeneity and plant species diversity: A hypothesis. *The American Naturalist*, *111*, 376–381.

Rüger, N., Comita, L. S., Condit, R., Purves, D., Rosenbaum, B., Visser, M. D., Joseph Wright, S., & Wirth, C. (2018). Beyond the fast–slow continuum: Demographic dimensions structuring a tropical tree community. *Ecology Letters, 21*, 1075–1084.

Rüger, N., Condit, R., Dent, D. H., DeWalt, S. J., Hubbell, S. P., Lichstein, J. W., Lopez, O. R., Wirth, C., & Farrior, C. E. (2020). Demographic trade-offs predict tropical forest dynamics. *Science, 368*, 165–168.

Rüger, N., Huth, A., Hubbell, S. P., & Condit, R. (2011). Determinants of mortality across a tropical lowland rainforest community. *Oikos, 120*, 1047–1056.

Rüger, N., Wirth, C., Wright, S. J., & Condit, R. (2012). Functional traits explain light and size response of growth rates in tropical tree species. *Ecology, 93*(12), 2626–2636.

Shipley, B., De Bello, F., Cornelissen, J. H. C., Laliberté, E., Laughlin, D. C., & Reich, P. B. (2016). Reinforcing loose foundation stones in trait-based plant ecology. *Oecologia, 180*, 923–931.

Silvertown, J. (2004). Plant coexistence and the niche. *Trends in Ecology & Evolution, 19*, 605–611.

Srivastava, D. S., & Lawton, J. H. (1998). Why more productive sites have more species: An experimental test of theory using tree-hole communities. *The American Naturalist, 152*, 510–529.

Stark, S. C., Leitold, V., Wu, J. L., Hunter, M. O., de Castilho, C. V., Costa, F. R., McMahon, S. M., Parker, G. G., Shimabukuro, M. T., & Lefsky, M. A. (2012). Amazon forest carbon dynamics predicted by profiles of canopy leaf area and light environment. *Ecology Letters, 15*, 1406–1414.

Terborgh, J., Huanca Nuñez, N., Alvarez Loayza, P., & Cornejo Valverde, F. (2017). Gaps contribute tree diversity to a tropical floodplain forest. *Ecology, 98*, 2895–2903.

Turner, I. M. (2001). *The ecology of tree in the tropical rain forest*. Cambrige University Press.

Valladares, F., & Niinemets, Ü. (2008). Shade tolerance, a key plant feature of complex nature and consequences. *Annual Review of Ecology, Evolution and Systematics, 39*, 237–257.

West, G. B., Enquist, B. J., & Brown, J. H. (2009). A general quantitative theory of forest structure and dynamics. *Proceedings of the National Academy of Sciences of the United States of America, 106*, 7040–7045.

White, E. P., Enquist, B. J., & Green, J. L. (2008). On estimating the exponent of power-law frequency distributions. *Ecology, 89*, 905–912.

White, E. P., Ernest, S., Kerkhoff, A. J., & Enquist, B. J. (2007). Relationships between body size and abundance in ecology. *Trends in Ecology & Evolution, 22*, 323–330.

Whitmore, T. (1984). Gap size and species richness in tropical rain forests. *Biotropica, 16*, 239.

Whitmore, T. (1989). Canopy gaps and the two major groups of forest trees. *Ecology, 70*, 536–538.

Wirth, R., Weber, B., & Ryel, R. J. (2001). Spatial and temporal variability of canopy structure in a tropical moist forest. *Acta Oecologica, 22*, 235–244.

Wright, S. J., Kitajima, K., Kraft, N. J., Reich, P. B., Wright, I. J., Bunker, D. E., Condit, R., Dalling, J. W., Davies, S. J., & Díaz, S. (2010). Functional traits and the growth–mortality trade-off in tropical trees. *Ecology, 91*, 3664–3674.

Zhang, W.-P., Morris, E. C., Jia, X., Pan, S., & Wang, G.-X. (2015). Testing predictions of the energetic equivalence rule in forest communities. *Basic and Applied Ecology, 16*, 469–479.

SUPPORTING INFORMATION

Additional supporting information can be found online in the Supporting Information section at the end of this article.

Supporting Information S1. Supplemental methods and results.

Supporting Information S2. Results summary for mass growth, stem diameter growth, abundance, aboveground woody productivity, richness, abundance.